



Near-surface reduction of cavity ring-down spectroscopy detection sensitivity

Maosheng Zhao ^a, Edward H. Wahl ^a, Thomas G. Owano ^{a,*}, Craig C. Largent ^b,
Richard N. Zare ^c, Charles H. Kruger ^a

^a Department of Mechanical Engineering, Stanford University, Bldg. 520, Duena Street, Stanford, CA 94305-3032, USA

^b Department of Engineering Physics, Air Force Institute of Technology, Wright-Patterson AFB, OH 45433-7765, USA

^c Department of Chemistry, Stanford University, Stanford, CA 94305-5080, USA

Received 22 December 1999

Abstract

Cavity ring-down spectroscopy (CRDS) is a high-sensitivity technique used to measure the absolute concentrations of absorbing species. We have used CRDS to measure spatially dependent concentration profiles near a physical surface that obstructs the light path. A decrease in detection sensitivity resulting from interaction between the circulating cavity ring-down beam and the surface was observed. Simple calculations based on geometrical obstruction by the solid surface significantly underestimate the sensitivity loss, suggesting that diffraction is important. Calculations that include diffraction effects more closely agree with experimental data. © 2000 Published by Elsevier Science B.V. All rights reserved.

1. Introduction

Cavity ring-down spectroscopy (CRDS) is a high-sensitivity absorption technique that provides measurements of absolute concentrations of trace gas species [1–5]. Typically, CRDS is accomplished by coupling a pulsed or cw laser source into a high-finesse optical resonator (Fabry–Pérot cavity) that encloses a sample of interest. Under resonant conditions, the light that exits the cavity at one of the mirrors decays exponentially in time. The time constant that characterizes the exponential decay of the

emitted light is referred to as the ring-down lifetime τ given by:

$$\tau = \frac{t_r}{2[(1 - \mathcal{R}) + \alpha l_s]}, \quad (1)$$

where t_r is the round-trip time of a light pulse in the cavity, $(1 - \mathcal{R})$ denotes the reflection loss for the cavity mirrors of reflectivity \mathcal{R} , and $2\alpha l_s$ is the round-trip absorbance for a sample present in the cavity with absorption coefficient α and path length l_s . Thus, a plot of $1/\tau$ as a function of wavelength gives the absorption spectrum, from which the absolute sample concentration can be determined, given a knowledge of the sample's absorption cross-section and path length. The sensitivity limit of CRDS can

* Corresponding author. Fax +1-650-723-1748; e-mail: owano@stanford.edu

be expressed as the minimum detectable absorbance per pass

$$(\alpha l_s)_{\min} = (1 - \mathcal{R}) \frac{\Delta\tau}{\tau}, \quad (2)$$

where $\Delta\tau/\tau$ is the minimum detectable change in the measured ring-down lifetime (typically 0.1–1% for typical detection electronics). This technique has been used extensively to perform absorption spectroscopy whenever high sensitivity and absolute concentration measurements are required.

In particular, we have used CRDS to measure the concentrations of gas species in reaction chambers where diamond films are grown by chemical vapor deposition (CVD) in either a plasma-activated or a hot-filament reactor. Specifically, we measured the concentration of various hydrocarbon species, such as CH and CH₃, as a function of distance from a metal surface, the deposition substrate in the case of the plasma-activated reactor and the filament in the case of the hot-filament reactor. In the course of these mechanistic studies, we observed that the presence of the surface in the optical cavity markedly reduced the sensitivity of the absorption measurement as the ring-down beam approached the surface. This sensitivity loss is the subject of this Letter.

2. Experimental measurements

The resonator geometry utilized for both setups consists of two mirrors of equal radius of curvature, R , separated by a distance, l , for which the circulating TEM₀₀ beam waist, ω_0 , is given by

$$\omega_0 = \left[\frac{\lambda\sqrt{l}}{2\pi} \sqrt{2R-l} \right]^{1/2}, \quad (3)$$

where λ is the laser wavelength. In both setups, the cavity was aligned longitudinally such that the position of the beam waist is coincident with the obstructing surface. A schematic diagram of the pertinent portion of both CVD reactors is shown in Fig. 1. Additional experimental setup parameters are given in Table 1.

Fig. 2 shows ring-down lifetimes collected using the hot-filament reactor. The normalized ring-down

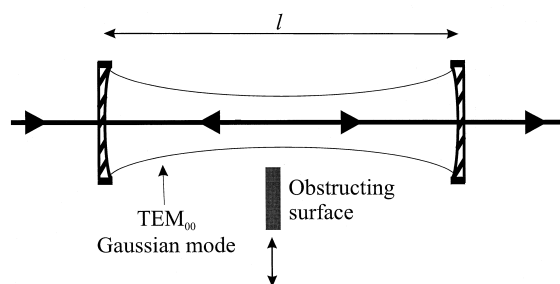


Fig. 1. Schematic of ring-down cavity used to characterize the spatially dependent concentrations of species in a CVD diamond reactor. The resonator formed by two mirrors of equal radius of curvature supports the TEM₀₀ Gaussian mode. The obstructing surface is translated laterally with respect to the ring-down beam.

lifetime is plotted versus the normalized distance from the center of the optical mode to the edge of the surface. These measurements (indicated by \bullet) were made with no absorbing species present in the chamber, so all losses result from either the mirrors or a combination of clipping and diffraction. For positions at which the beam is far from the filament, the ring-down lifetime is unaffected by the presence of the surface and is equal to the empty-cavity ring-down lifetime (τ_0). As the distance between the beam and the filament is decreased, the ring-down lifetime decreases as additional loss is introduced.

The dashed curve in Fig. 2 is the normalized ring-down lifetime calculated from strictly geometrical clipping (described below). As can be seen, this calculation significantly underestimates the reduction in normalized ring-down lifetime. For example, at two beam waists away from the surface, the actual ring-down lifetime has been reduced to 5% of τ_0 , although the geometrical clipping calculation predicts practically no decrease. The solid curve in Fig. 2 is the normalized ring-down lifetime calculated using a more detailed model (described below) that incorporates diffraction effects. It agrees much more closely with the experimental data.

Fig. 2 illustrates the detection sensitivity limitations inherent in using CRDS to measure spatially dependent concentration profiles in proximity to surfaces. As the measurement position moves closer to the surface, the normalized ring-down lifetime decreases, which results in a corresponding decrease in

Table 1
CRDS resonator parameters

Parameter	Hot-filament reactor	Plasma-activated reactor
Cavity length, d (m)	0.65	1.12
Mirror radius, R (m)	6	6
Wavelength, λ (nm)	430	437
Beam waist, ω_0 (mm)	0.431	0.493
Mirror reflectivity, \mathcal{R}	0.9999	0.999
Empty-cavity ring-down lifetime, τ_0 (μs)	43	4.43

detection sensitivity. For the previous example of the hot-filament reactor, at two beam waists away from the surface, the actual ring-down lifetime has been reduced to 5% of τ_0 , and the minimum detectable absorbance has increased by a factor of 20.

Fig. 3 shows the ring-down lifetime as a function of distance for the case of the plasma-activated CVD reactor. As in the case of the hot-filament reactor, the measured ring-down lifetime (indicated as \bullet) decreases as the surface approaches the circulating ring-down beam. The case of the plasma-activated reactor demonstrates the additional impact of decreased mirror reflectivity on sensitivity reduction. In this case, the mirror reflectivity ($R = 99.9\%$) yields a mirror loss ($1 - R = 0.1\%$) one order of magnitude higher than the mirror loss ($1 - R = 0.01\%$) for the hot-filament reactor ($R = 99.99\%$). The minimum detectable absorbance is thus an order of magnitude

higher (as evidenced by the empty-cavity ring-down lifetimes in Table 1). Fig. 3 shows that this reduction in mirror reflectivity results in a smaller impact on the normalized sensitivity at a given measurement position. For example, at two beam waists away from the surface, the actual ring-down lifetime has only been reduced to 35% of τ_0 , and the minimum detectable absorbance becomes a factor of 3 higher. Although the use of low-reflectivity mirrors results in smaller reductions in normalized sensitivity for a given measurement position, it should be noted that low-reflectivity mirrors also provide lower absolute sensitivity. Therefore, it is logical that the losses caused by the presence of a surface in the ring-down cavity would not be observed until smaller distances are approached, and the magnitude of surface-induced losses become comparable to the losses at the mirrors.

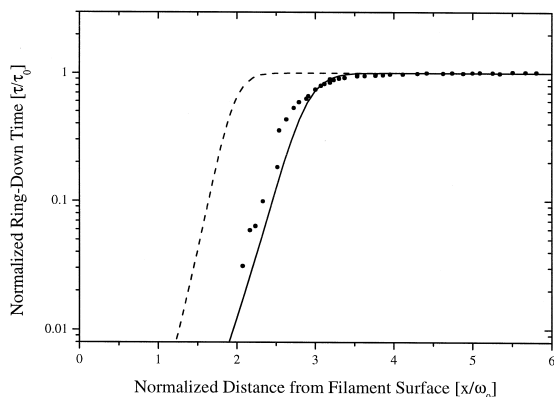


Fig. 2. Normalized ring-down lifetime vs. normalized distance from filament to beam center for the hot-filament reactor. Detection sensitivity decreases with decreasing distance between the filament and ring-down beam. Mirror reflectivity = 99.99%.

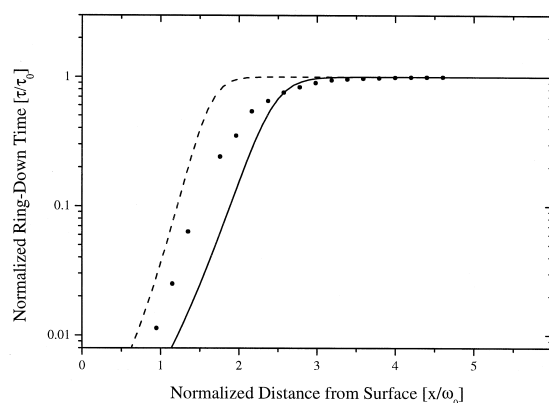


Fig. 3. Normalized ring-down lifetime vs. normalized distance from substrate to beam center for the plasma activated CVD reactor. Mirror reflectivity = 99.9%.

3. Theory

In order to calculate the impact of a surface on the ring-down lifetime, we modified Eq. (1) to include an additional spatially dependent loss term:

$$\tau(d) = \frac{t_r}{2[(1 - \mathcal{R}) + \alpha l_s + \alpha_c(d)]}, \quad (4)$$

where $\alpha_c(d)$ is the spatially dependent absorbance per pass caused by interaction with the surface inside the optical resonator. Accordingly, the minimum detectable absorbance per pass is now given by:

$$(\alpha l_s)_{\min} = [(1 - \mathcal{R}) + \alpha_c(d)] \frac{\Delta\tau}{\tau}. \quad (5)$$

The optical mode supported by the resonator used in these experiments is the Gaussian TEM₀₀ mode. At the beam waist (the location of the surface in our experimental setups), this mode is described by the electric field,

$$\begin{aligned} \bar{E} &= E_0 \exp(-d^2/\omega_0^2) \\ &= E_0 \exp\left[-\left(\sqrt{x^2 + y^2}\right)^2/\omega_0^2\right], \end{aligned} \quad (6)$$

where d is the distance from the center of the beam to the position of interest.

To evaluate the fraction of the beam that is simply geometrically clipped by the surface, the optical intensity profile was integrated over the dimensions of the surface. We found that regardless of whether this integration was performed over only the dimensions of the finite-width filament (x_1 to x_2) or from the edge of the surface (x_1) to infinity, the difference in the result was negligible. Therefore, we utilized the latter method of integration in our results:

$$\begin{aligned} \alpha_c &= \frac{\int_{y=0}^{\infty} \int_{x=x_1}^{\infty} I(x, y) dx dy}{\int_0^{\infty} \int_0^{\infty} I(x, y) dx dy} \\ &= \frac{\int_{y=0}^{\infty} \int_{x=x_1}^{\infty} E_0^2 \exp[-(x^2 + y^2)/\omega_0^2] dx dy}{\int_0^{\infty} \int_0^{\infty} E_0^2 \exp[-(x^2 + y^2)/\omega_0^2] dx dy} \\ &= \frac{1}{2} \left[1 - \operatorname{erf}\left(\frac{\sqrt{2} x_1}{\omega_0}\right) \right]. \end{aligned} \quad (7)$$

The dashed curves shown in Figs. 2 and 3 are calculated using Eq. (7).

A more accurate model of the surface-induced losses must also incorporate the effects of diffraction occurring at the edge of the surface. Using the results of Pearson et al. [6], who developed general expressions for the diffraction of a Gaussian beam by a semi-infinite plane, we derived a more accurate expression for the surface losses. By assuming the surface to be a semi-infinite plane located at the beam waist, we evaluated the normalized farfield decrease in centerline field magnitude as a function of distance from the edge of the half-plane to the center of the beam waist. We assumed this loss to be equal to the single-pass loss of a circulating ring-down beam. Although this assumption is approximate at best, it represents a tractable solution to what is otherwise an extremely complicated series of individual diffraction problems. It should also be pointed out that this approximation does not consider the diffraction of beam energy into higher-order transverse modes. Nonetheless, the results of calculating the surface induced losses in this manner (shown by the solid lines in Figs. 2 and 3) are in relatively good agreement with the experimental data. Moreover, the quality of this agreement indicates that diffraction is a primary loss mechanism at large distances. This method can then be utilized for deriving more general experimental design parameters.

4. Circular apertures

Although the case of an axisymmetric surface (such as a limiting aperture or iris diaphragm) was not experimentally considered, the loss expressions are much more straightforward than for the obstructing half-plane, and are provided for reference. For the geometric clipping losses [7]

$$\alpha_c(r) = \exp\left[-2\frac{r^2}{\omega_0^2}\right], \quad (8)$$

where r is the radius of the aperture. For the losses including diffraction effects [7]

$$\alpha_c(r) = \left\{ 1 - \left[1 - \exp\left(\frac{-r^2}{\omega_0^2}\right) \right]^2 \right\}. \quad (9)$$

5. Experimental design considerations

By making use of our half-plane diffraction model, we have performed calculations to aid in the design of CRDS experiments in which the circulating beam comes close to surfaces inside the optical cavity. Fig. 4 provides experimental design constraints for performing spatially resolved CRDS in near-surface environments. In the figure, we plot the normalized ring-down lifetime as a function of mirror reflectivity and normalized beam position. Use of this figure provides quantitative data relating maximum sensitivity loss and the choice of mirror reflectivity to the minimum proximity to surfaces in the cavity. For example, if the maximum sensitivity loss that can be tolerated is 10% ($\tau/\tau_0 = 0.9$), then the use of mirrors with 99.9% reflectivity will require measurements to be made farther than 2.7 beam waists from the surface.

One possible solution to overcoming these spatial sensitivity limitations is to decrease the beam waist inside the ring-down cavity, which would allow for increased sensitivity at a given distance. To examine the possibility of reducing the beam waist in our ring-down cavities, we have plotted in Fig. 5 the beam waist as a function of mirror radius of curva-

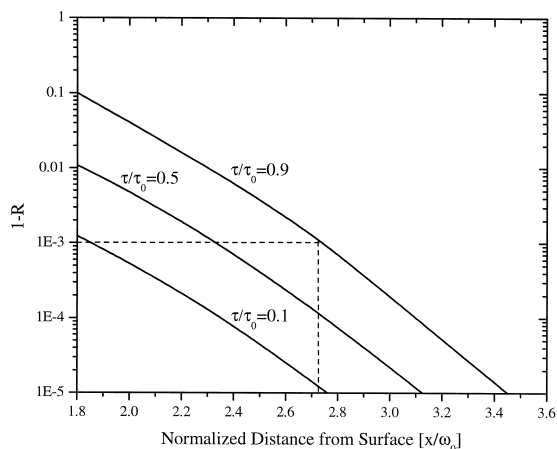


Fig. 4. Experimental design curves for spatially dependent CRDS experiments. The dashed lines represent a design constraint given a mirror reflectivity of 99.9% and maximum sensitivity loss of 10%, resulting in a minimum proximity of ~ 2.7 beam waists. Given a mirror reflectivity, and desired ring-down lifetime ratio, the minimum normalized distance from surface to beam can be determined.

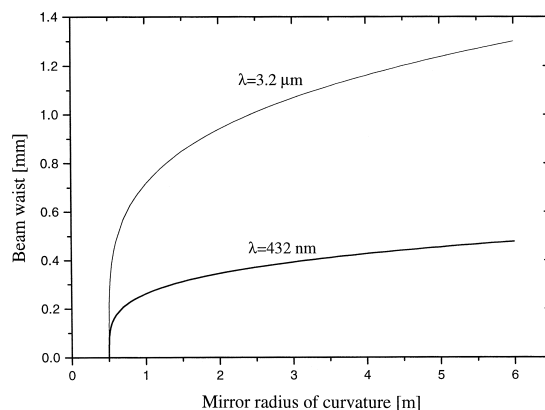


Fig. 5. Beam waist as a function of mirror radius of curvature. A cavity length of 1 m is assumed for the calculation.

ture, assuming a resonator with two mirrors of equal radius of curvature and a cavity length of 1 m. Such a resonator is stable over a range of curvatures but does not experience a significant reduction in the beam waist until the geometry is close to the concentric configuration (cavity length = $2R$). Unfortunately, close to this configuration, the resonator is on the edge of stability. We have found that operation at cavity lengths greater than $1.8R$ results in instability from small fluctuations in cavity geometry. Therefore, for the case of a 432 nm laser, the minimum beam waist is constrained to be greater than 0.2 mm in size.

Another technique that will reduce CRDS sensitivity limitations is to decrease the laser wavelength. We have performed CRDS experiments using an IR OPO at $3.2 \mu\text{m}$ [8] and have plotted the corresponding waist size in Fig. 5. As we expected, the decrease in sensitivity was more pronounced at these longer wavelengths.

6. Conclusions

We have observed a decrease in CRDS detection sensitivity resulting from interaction between the circulating cavity ring-down beam and an intercavity surface. Simple calculations based on geometrical obstruction by the solid surface significantly underestimate the sensitivity loss, whereas calculations

that include diffraction effects more closely agree with experimental data. These results provide guidelines for design of spatially resolved CRDS experiments in which surfaces are present inside the optical cavity.

Acknowledgements

This work was supported by the Engineering Research Program of the Office of Basic Energy Sciences at the US Department of Energy, and by the Director of Defense Research and Engineering (DDR &E) within the Air Plasma Ramparts MURI program managed by the Air Force Office of Scientific Research.

References

- [1] D. Romanini, K.K. Lehmann, *J. Chem. Phys.* 99 (1993) 6287.
- [2] P. Zalicki, R.N. Zare, *J. Chem. Phys.* 102 (1995) 2708.
- [3] A. O'Keefe, J.J. Scherer, A.L. Cooksy, R. Sheeks, J. Heath, R.J. Saykally, *Chem. Phys. Lett.* 172 (1990) 214.
- [4] G. Meijer, M.G.H. Boogaarts, R.T. Jongma, D.H. Parker, A.M. Wodtke, *Chem. Phys. Lett.* 217 (1994) 112.
- [5] B.A. Paldus, C.C. Harb, T.G. Spence, B. Wilke, J. Xie, J.S. Harris, R.N. Zare, *J. Appl. Phys.* 83 (1998) 3991.
- [6] J.E. Pearson, T.C. McGill, S. Kurtin, A. Yariv, *J. Opt. Soc. Am.* 59 (1969) 1440.
- [7] A.E. Siegman, *Lasers*, University Science Books, Mill Valley, CA, 1986.
- [8] J. Martin, B.A. Paldus, P. Zalicki, E.H. Wahl, T.G. Owano, J.S. Harris Jr., H. Kruger, R.N. Zare, *Chem. Phys. Lett.* 258 (1996) 63.